

Interfacial Electrical Properties of DNA-Modified Diamond Thin Films: Intrinsic Response and Hybridization-Induced Field Effects

Wensha Yang,[†] James E. Butler,[‡] John N. Russell, Jr.,[‡] and Robert J. Hamers^{*,†}

Department of Chemistry, University of Wisconsin—Madison, 1101 University Avenue, Madison, Wisconsin 53706, and Chemistry Division, Naval Research Laboratory, 4555 Overlook Avenue S.W., Washington, D.C. 20375

Received December 27, 2003. In Final Form: May 11, 2004

We have investigated the frequency-dependent interfacial electrical properties of nanocrystalline diamond films that were covalently linked to DNA oligonucleotides and how these properties are changed upon exposure to complementary and noncomplementary DNA oligonucleotides. Frequency-dependent electrical measurements at the open-circuit potential show significant changes in impedance at frequencies of $>10^4$ Hz when DNA-modified diamond films are exposed to complementary DNA, with only minimal changes when exposed to noncomplementary DNA molecules. Measurements as a function of potential show that at 10^5 Hz, the impedance is dominated by the space-charge region of the diamond film. DNA molecules hybridizing at the interface induce a field effect in the diamond space-charge layer, altering the impedance of the diamond film. By identifying a range of impedances where the impedance is dominated by the diamond space-charge layer, we show that it is possible to directly observe DNA hybridization, in real time and without additional labels, via simple measurement of the interfacial impedance.

Introduction

Recent advances in areas such as molecular electronics and biological sensing have placed increased emphasis on understanding the electrical properties of molecules and molecular layers on surfaces.^{1,2} The detection of biological binding events such as DNA hybridization and/or protein binding at surfaces is of central importance in modern biomedical sciences through a variety of “biochip” devices, lending particular importance to biologically modified surfaces.^{2,3} Gold^{4–12} and silicon^{13–18} have been especially widely used as model systems for understanding

structural and electrical properties of monolayer systems. Silicon has been heavily studied because of the possibility of fabricating field-effect devices, analogous to field-effect transistors but with chemical and/or biochemical sensitivity.^{18–21} Field-effect devices are also particularly attractive for converting biological information directly into electrical signals because these devices are essentially sensitive to the presence of electrical charge. Since the vast majority of biomolecules are charged, this means that the use of the field effect can be a very general method for detecting a wide variety of biomolecules, provided that the proper biomolecular binding sites can be attached to a surface.^{15–17,19–21} Indeed, we have recently shown that on DNA-modified silicon surfaces, hybridization of complementary DNA to the surface-tethered oligonucleotides induces changes in impedance due to a field effect, in which the negatively charged DNA molecules affect the properties of the semiconductor space-charge layer, increasing the impedance on n-type substrates and decreasing the impedance on p-type substrates.²²

Diamond is an attractive material as a substrate for biological modification because it has very good chemical and electrochemical stability and a large (5.5 eV) band gap.^{23–30} While the electrical properties of clean and

* Corresponding author. Phone: 608-262-6371. Fax: 608-262-0453. E-mail: rjhamers@facstaff.wisc.edu.

[†] University of Wisconsin—Madison.

[‡] Naval Research Laboratory.

(1) *Molecular Electronics II*; Aviram, A.; Ratner, M.; Mujica, V., Mujico, V., Eds.; New York Academy of Sciences: New York, 2003.

(2) *Electroanalytical Methods for Biological Materials*; Brajter-Toth, A.; Chamber, J. Q., Eds.; Marcel Dekker: New York, 2002.

(3) *Biochips: Technology and Applications*; Xing, W.-L., Cheng, J., Eds.; Springer-Verlag: Berlin, 2003.

(4) Laibinis, P. D.; Whitesides, G. M.; Allara, D. L.; Tao, Y.-T.; Parikh, A. N.; Nuzzo, R. G. *J. Am. Chem. Soc.* **1991**, *113*, 7152.

(5) Finklea, H. O.; Hanshew, D. D. *J. Am. Chem. Soc.* **1992**, *114*, 3173.

(6) Miller, C.; Graetzel, M. *J. Phys. Chem.* **1991**, *95*, 5225.

(7) Miller, C.; Cuendet, P.; Graetzel, M. *J. Phys. Chem.* **1991**, *95*, 877.

(8) Lee, M.-T.; Hsueh, C.-C.; Freund, M. S.; Ferguson, G. S. *Langmuir* **1998**, *14*, 6419.

(9) Flynn, N. T.; Tran, T. N. T.; Cima, M. J.; Langer, R. *Langmuir* **2003**, *19*, 10909.

(10) Herne, T. M.; Tarlov, M. *J. Am. Chem. Soc.* **1997**, *119*, 8916.

(11) Steel, A. B.; Herne, T.; Tarlov, M. *J. Anal. Chem.* **1998**, *70*, 4670.

(12) Kelley, S. O.; Boon, E. M.; Barton, J. K.; Jackson, N. M.; Hill, M. G. *Nucleic Acids Res.* **1999**, *27*, 4830.

(13) Buriak, J. M. *Chem. Rev.* **2002**, *102*, 1271.

(14) Linford, M. R.; Fenter, P.; Eisenberger, P. M.; Chidsey, C. E. D. *J. Am. Chem. Soc.* **1995**, *117*, 3145.

(15) Webb, L. J.; Lewis, N. S. *J. Phys. Chem. B* **2003**, *107*, 5404.

(16) Allongue, P.; de Villeneuve, C. H.; Pinson, J. *Electrochim. Acta* **2000**, *45*, 3241.

(17) Barrelet, C. J.; Robinson, D. B.; Cheng, J.; Hunt, T. P.; Quate, C. F.; Chidsey, C. E. D. *Langmuir* **2001**, *17*, 3460.

(18) Wei, F.; Sun, B.; Guo, Y.; Zhao, X. S. *Biosens. Bioelectron.* **2003**, *18*, 1157.

(19) Fritz, J.; Cooper, E. B.; Gaudet, S.; Sorger, P. K.; Manalis, S. R. *Proc. Natl. Acad. Sci. U.S.A.* **2002**, *99*, 14142.

(20) Souteyrand, E.; Cloarec, J. P.; Martin, J. R.; Wilson, C.; Lawrence, I.; Mikkelsen, S.; Lawrence, M. F. *J. Phys. Chem. B* **1997**, *101*, 2980.

(21) Souteyrand, E.; Martin, J. R.; Martelet, C. *Sens. Actuators, B* **1994**, *20*, 63.

(22) Cai, W.; Peck, J.; van der Weide, D.; Hamers, R. J. *Biosens. Bioelectron.* **2004**, *19*, 1013.

(23) Yang, W.; Butler, J. E.; Cai, W.; Carlisle, J.; Gruen, D.; Knickerbocker, T.; Russell, J. N., Jr.; Smith, L. M.; Hamers, R. J. *Nat. Mater.* **2002**, *1*, 253.

(24) Knickerbocker, T.; Strother, T.; Schwartz, M. P.; Russell, J. N., Jr.; Butler, J. E.; Smith, L. E.; Hamers, R. J. *Langmuir* **2003**, *19*, 1938.

(25) Yang, W.; Auciello, O.; Butler, J. E.; Cai, W.; Carlisle, J.; Gerbi, J. E.; Gruen, D. M.; Knickerbocker, T.; Lasseter, T. L.; Russell, J. N., Jr.; Smith, L. M.; Hamers, R. J. *Mater. Res. Soc. Symp. Proc.* **2003**, *737*, F4.4.1.

(26) Granger, M. C.; Swain, G. M. *J. Electrochem. Soc.* **1999**, *146*, 4551.

hydrogen-terminated diamond films have been extensively investigated, comparatively little work has been done on the properties of diamond surfaces after modification with molecular or biomolecular films. Indeed, the high intrinsic stability of the diamond surface makes it a difficult surface to functionalize.

We have recently developed a photochemical method for covalently linking organic molecules to the surfaces of diamond thin films and have used this method as a starting point for covalently linking DNA oligonucleotides to diamond surfaces. Those experiments showed that DNA-modified diamond surfaces showed good biological selectivity and outstanding chemical stability when subjected to repeated cycles of hybridization and denaturation.^{23–25} Here, we report investigations of the electrical properties of DNA-modified diamond surfaces and how these electrical properties are affected by exposure to complementary and noncomplementary DNA sequences in solution. Our results demonstrate the potential for using electrical impedance measurements as a means to detect biological binding events in real time as a consequence of the field effect induced in the diamond by the charged DNA molecules.

Experimental Methods

Growth of Diamond Thin Films. All samples used here were boron-doped (p-type) nanocrystalline diamond thin films approximately 0.5 μm thick, grown on p-type Si(100) substrates at the Naval Research Laboratory in a 2.45 GHz microwave plasma reactor (Astex model PDS-17) using purified hydrogen (900 sccm) and methane (3 sccm), with a doping concentration of approximately 10^{18} cm^{-3} .³¹ Figure 1a shows a scanning electron microscope image of a typical film after cleaning and functionalization as described below. High-resolution images show a highly faceted surface structure with grain sizes ranging from ~ 20 to 50 nm.

Cleaning and Functionalization. Figure 1b shows an outline of the chemical attachment scheme, which has been described previously.²³ The diamond films were cleaned and terminated with hydrogen by heating the sample to 700 °C in a 13.56 MHz inductively coupled hydrogen plasma (20 Torr) for 20 min and then cooling to room temperature before extinguishing the plasma.³² X-ray photoelectron spectra on these samples showed a single, sharp C(1s) peak with no detectable O(1s) and no detectable forms of oxidized carbon, consistent with previous studies.^{23–25,33} The H-terminated samples were functionalized with amine groups using 10-aminodec-1-ene that was protected with the trifluoroacetic acid group (see Figure 1). A small drop of this liquid was placed upon the H-terminated samples, directly covered with a quartz coverslip, and illuminated through the coverslip with ultraviolet light from a low-pressure mercury lamp (254 nm, 0.35 mW/cm²) for 12 h under dry nitrogen. This procedure links the protected amine to the diamond surface through the vinyl group.³³ Core-level photoemission measurements on nanocrystalline,²³ microcrystalline,^{23,33} and single-crystal (111) diamond³⁴ under the conditions used here show similar reaction efficiency, demonstrating that the chemistry is not strongly dependent on the surface morphology. The modified samples were immersed into 0.36 M HCl in methanol for 24 h at 65 °C to deprotect the amine, yielding diamond surfaces

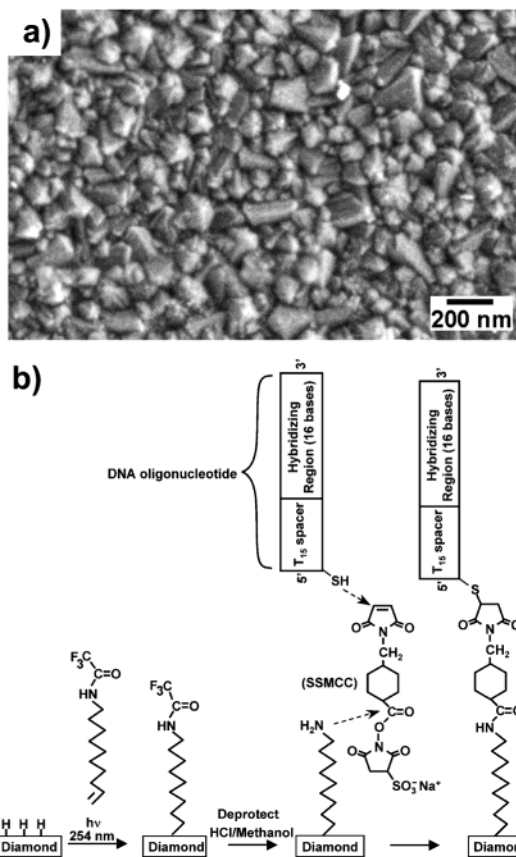


Figure 1. (a) Scanning electron microscope image of modified diamond thin film. (b) Schematic illustration of the procedure used to covalently link DNA to the diamond surface.

terminated with a molecular layer exhibiting a high density of exposed free primary amine groups.²³

Covalent Linking of DNA Oligonucleotides. To link DNA to the exposed amine groups, the amine-modified diamond surfaces were exposed to a 1 mM solution of the heterobifunctional cross-linker sulfo-succinimidyl 4-(*N*-maleimidomethyl) cyclohexane-1-carboxylate (SSMCC) in triethanolamine buffer solution (pH 7) for 20 min; the DNA oligonucleotides modified with a thiol group at the 5' end were then linked to this surface by applying 10 μL of 250 μM thio-oligonucleotide and keeping the sample in a humid reaction vessel for at least 6 h. Previous studies have shown that this procedure yields DNA-modified surfaces that are extremely stable and that exhibit high selectivity toward complementary versus noncomplementary sequences.^{23,35}

In our experiments, the DNA molecules that are attached to the surface are 31 bases long with the sequence 5'-HS-C₆H₁₂-T₁₅-GCTTAAGGAGCAATCG-3'; this sequence (denoted S1) includes a thiol group for linking to the surface, a six-carbon alkyl chain, a repeated sequence of 15 thymine groups that acts as a spacer, and a sequence of 16 bases that can hybridize with complementary sequences introduced in solution. The solution-phase oligonucleotides used to test the hybridization were modified with the fluorescent label fluorescein phosphoramidite (FAM). Two types of solution-phase DNA were used: the perfectly matched complementary DNA with the sequence 5'-FAM-CGATTGCTCCTTAAGC-3' (F1) and the 4-base mismatched DNA with the sequence 5'-FAM-CGAAAGCTCGATAAGC-3' (F2). While the data shown here were obtained using fluorescein-labeled oligonucleotides, electrical measurements were also made using oligonucleotides without fluorescent labels. Those experiments yielded the same electrical properties as those reported here, leading us to conclude that the fluorescent labels do not significantly affect the electrical measurements.

(27) Granger, M. C.; Witek, M.; Xu, J. S.; Wang, J.; Hupert, M.; Hanks, A.; Koppang, M. D.; Butler, J. E.; Lucazeau, G.; Mermoux, M.; Strojek, J. W.; Swain, G. M. *Anal. Chem.* **2000**, *72*, 3793.

(28) Kuo, T. C.; McCreery, R. L.; Swain, G. M. *Electrochem. Solid State Lett.* **1999**, *2*, 288.

(29) Show, Y.; Witek, M.; Sonthalia, P.; Swain, G. M. *Chem. Mater.* **2003**, *15*, 879.

(30) Swain, G. M.; Ramesham, M. *Anal. Chem.* **1993**, *65*, 345.

(31) Butler, J. E.; Windischmann, H. *MRS Bull.* **1998**, *23*, 22.

(32) Thoms, B. D.; Owens, M. S.; Butler, J. E.; Spiro, C. *Appl. Phys. Lett.* **1994**, *65*, 2957.

(33) Strother, T.; Knickerbocker, T.; Russell, J. N., Jr.; Butler, J. E.; Smith, L. M.; Hamers, R. J. *Langmuir* **2002**, *18*, 968.

(34) Nichols, B.; Yang, W.; Hamers, R. J. In preparation, 2003.

(35) Strother, T.; Hamers, R. J.; Smith, L. M. *Nucleic Acids Res.* **2000**, *28*, 3535.

Electrical Characterization. Electrochemical measurements were performed in a thin three-electrode electrochemical flow cell. In this cell, the DNA-modified diamond sample acts as a working electrode and a Pt foil acts as a counter electrode. These planar electrodes are separated by a thin sheet of poly-(dimethylsiloxane) (PDMS) with a 3 mm × 1.5 mm opening that forms a fluid cavity with a volume of 4.5 μ L. The Pt foil (counter electrode) and the DNA-modified diamond (working electrode) press against the PDMS to seal the top and bottom of the cell. A reference electrode (Ag/AgCl) was made using a 25 μ m diameter Ag wire coated with AgCl, which was then embedded into the PDMS with approximately 3 mm exposed to the solution. Microfluidic inlet and outlets were also embedded into the PDMS to permit solutions to be flowed continuously through the cell using a syringe pump.

Electrochemical measurements were performed using a three-electrode potentiostat (Solartron 1260) and impedance analyzer (Solartron 1287) using Corrware and Zplot software (Scribner Associates, Inc). Cyclic voltammetry measurements were performed in a redox solution (RS) using a solution of 0.5 mM $\text{Fe}(\text{CN})_6^{3-}$, 0.5 mM $\text{Fe}(\text{CN})_6^{4-}$, 100 mM KCl, and 100 mM KNO_3 at a scan rate of 200 mV/s. Impedance measurements were obtained in a standard hybridization buffer (HB) solution consisting of 300 mM NaCl, 20 mM sodium phosphate, 2 mM EDTA, and 6.9 mM sodium dodecyl sulfate, without any redox couple added. All electrical measurements were performed with the solution of interest flowing at a rate of 0.1 mL/min.

Results

Cyclic Voltammetry. Figure 2a shows a cyclic voltammogram (CV) of a H-terminated p-type diamond sample in the redox solution RS. The H-terminated diamond exhibits a clear oxidation wave with a maximum at 250 mV (vs Ag/AgCl reference electrode) and a corresponding reduction wave with a peak near zero volts, due to the redox reaction $\text{Fe}(\text{CN})_6^{3-} + e^- \rightarrow \text{Fe}(\text{CN})_6^{4-}$. This behavior is similar to that reported previously on polycrystalline p-type diamond electrodes.^{29,30} The presence of clear oxidation and reduction waves and the overall magnitude of the current indicate that electron transfer is facile on the H-terminated sample. Previous studies have established that diamond has a very wide range of electrochemical stability.²⁷ Our experiments confirm very stable electrochemical properties with facile electron transfer on diamond surfaces that have not yet been functionalized with organic layers.

Figure 2b shows a voltammogram of an identical sample that was covalently linked to a DNA oligonucleotide with sequence S1 (S1-DNA-diamond) as described above. While the H-terminated sample yielded oxidation and reduction peaks with $> 200 \mu\text{A}/\text{cm}^2$ peak current density, after linking to single-stranded DNA the voltammogram (solid line) shows that this current flow is drastically reduced to $1 \mu\text{A}/\text{cm}^2$ at this same potential. The absence of any peaks suggests that this residual current flow is primarily capacitive, with some conductivity arising from diffusion through the molecular layer.

After this voltammogram was obtained, a solution containing fluorescently labeled complementary DNA (F1) was injected into the cell for 30 min, and the cell was then rinsed with hybridization buffer to eliminate excess DNA and return the electrolyte to a constant composition. The cyclic voltammogram (Figure 2b, dashed line) is nearly identical to that of the surface that was not exposed to complementary DNA, except for a very small increase in the current at the maximum positive and negative potentials.

To verify that the samples exposed to DNA did indeed hybridize, fluorescence images were obtained of samples exposed to complementary DNA. Figure 2c shows a representative fluorescence image. The rectangular region

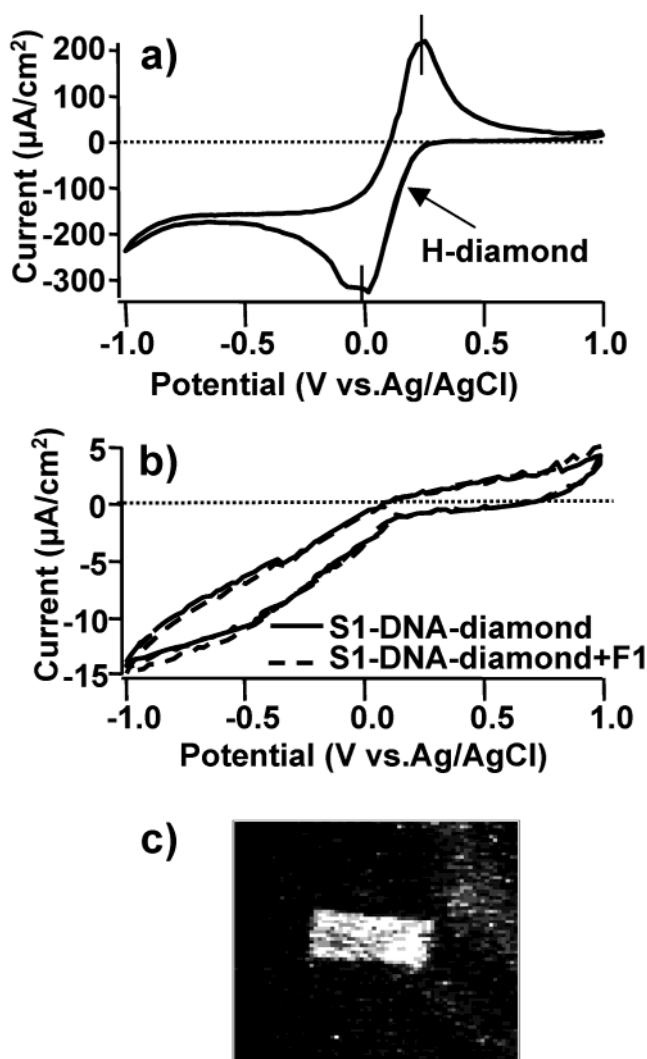


Figure 2. Cyclic voltammograms of H-terminated and DNA-modified diamond thin films. (a) Cyclic voltammogram on H-terminated diamond, showing reversible oxidation–reduction peaks. (b) Cyclic voltammogram on DNA-modified diamond before and after hybridization with complementary sequence F1, showing the blocking induced by the molecular layers and the lack of sensitivity to DNA hybridization. (c) Fluorescence image (bright = high intensity) after the DNA-modified surface was hybridized with complementary sequence F1. The small square shows the region where the sample was exposed in the fluid.

of the sample that was exposed to complementary DNA shows high fluorescence intensity, while the rest of the sample that was not exposed to the complementary DNA shows almost no intensity. Similar fluorescence measurements made on a number of other samples exposed to complementary and noncomplementary DNA confirmed that the fluorescence arises from specific hybridization between complementary DNA sequences with almost no nonspecific binding, consistent with previous results.^{23,24} Fluorescence measurements made before and after cyclic voltammogram sweeps showed that there was no significant change in intensity induced by the CV measurement at potentials between -1.0 and $+1.0$ V versus Ag/AgCl. Thus, under the conditions used here the cyclic voltammetry experiment does not denature the surface-hybridized DNA.

The sharp reduction in current upon attachment of single-stranded DNA to the surface shows that the molecular layers effectively insulate the diamond sub-

strate from the electrolyte solution, blocking almost all direct electron transfer even when the surface-tethered DNA is hybridized with its complementary sequence. While previous studies have shown that the intrinsic conductivity of DNA changes as a result of hybridization,^{12,36,37} the ability to observe this via cyclic voltammetry is inhibited by the highly insulating nature of the molecular scaffolding linking the DNA molecule to the underlying substrate.

Impedance Spectroscopy of DNA-Modified Diamond Surfaces. While the molecular layers appear to strongly inhibit electron transfer, more detailed information about the electrical properties of the interface can be obtained using electrical impedance spectroscopy. In impedance spectroscopy, the potential of the sample is modulated by a small sinusoidal excitation signal (typically 10 mV root-mean-square), and the in-phase and out-of-phase components of the current at the excitation frequency f_{mod} are measured. Measuring the in-phase and out-of-phase components of the current as the modulation frequency f_{mod} is swept over a wide range yields a complete frequency spectrum of the electrical response. Our impedance spectroscopy experiments are performed at the open-circuit potential with only a 10 mV modulation, in HB solution without any added redox agents. Under these conditions, there is no oxidation–reduction chemistry taking place, and the measurements are a very gentle way of measuring the intrinsic electrical properties of the interface. Because the current and voltage do not have the same phase and are frequency dependent, the impedance (Z) and its inverse, the admittance (Y), are usually described as complex, frequency-dependent quantities. The complex impedance is defined as $\hat{Z} = \hat{V}/\hat{I} = Z + iZ'$ and the complex admittance is defined as $\hat{Y} = 1/\hat{Z} = Y + iY'$, where $Y = Z/|\hat{Z}|^2$, and $Y' = -Z'/|\hat{Z}|^2$.

Figure 3a,b shows logarithmic plots of the real (Z) and imaginary (Z') impedances of a DNA-modified diamond surface (before hybridization) as a function of the applied electrochemical potential (vs Ag/AgCl reference) measured in 0.1 M KCl. The real and imaginary parts of the impedance vary by many orders of magnitude over the frequency range measured. At frequencies of less than ~ 1 kHz, Z and Z' are both nearly independent of the applied potential, while at higher frequencies the real and imaginary parts both increase as the applied potential is made more positive. The changes in impedance are somewhat more apparent in the real part of the impedance than in the imaginary part. The variation in impedance with applied electric potential is characteristic of a semiconductor interface and indicates that at frequencies of ~ 1 kHz the impedance is dominated by the space-charge layer of the diamond.^{20,21,38,39}

Figure 4a–d shows similar measurements of Z and Z' versus frequency for a different diamond thin film that was modified with (single-stranded) DNA and the change in response due to exposure to complementary and noncomplementary DNA in solution. Because the hybridization-induced changes in electrical properties are most apparent at high frequencies where the total impedance is small (vide infra), we also show these data in two alternate representations that emphasize these changes. Figure 4c shows a plot of the region highlighted in Figure 4a, highlighting the high-frequency behavior of

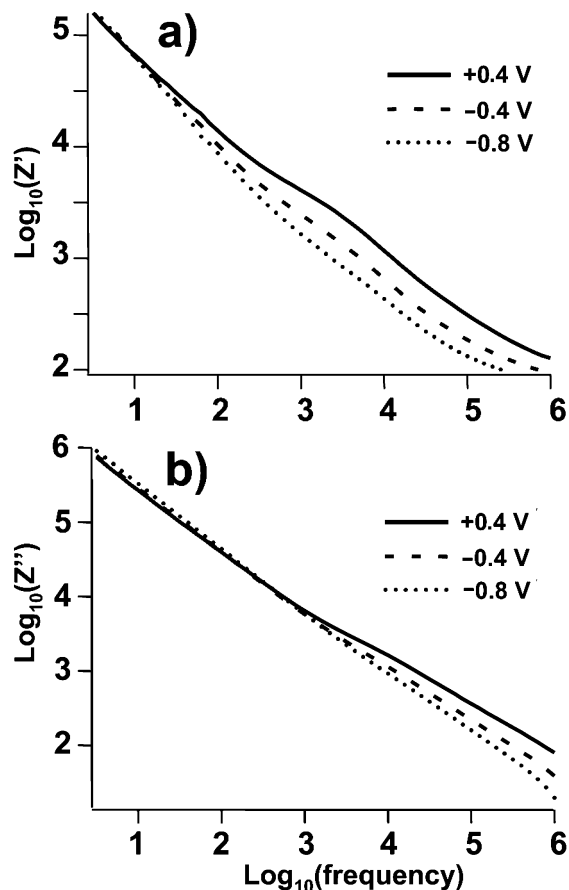


Figure 3. Impedance spectra of a DNA-modified diamond sample.

Z . Figure 4d shows a linear plot of the imaginary and real components of the admittance on a single plot, often referred to as a “Cole–Cole” plot.⁴⁰ To identify changes in impedance due to DNA hybridization, a solution containing 5 μM of the fluorescently labeled complement, F1, was then pumped through the cell for 20 min to permit the solution-phase DNA to hybridize with that on the surface. The cell was then flushed with HB solution for 10 min to eliminate any residual physically adsorbed DNA on the surface, and an impedance spectrum was measured. Comparison of the spectra before and after hybridization shows that the most apparent change is a decrease in the real component (Z) and a smaller decrease in the imaginary part (Z') of the impedance at high frequencies of >10 kHz. Although not striking when plotted on a logarithmic scale, the decreased Z is quite apparent at frequencies of >10 kHz, and at the highest frequencies measured corresponds to a change by more than a factor of 2 (a decrease from 133 to 57 Ω at 1.6 MHz). The hybridization-induced changes in Z and Z' at high frequency can be observed clearly in the Cole–Cole plot shown in Figure 4d. In addition to the changes at high frequency, hybridization also induces a smaller change at very low frequencies (<1 Hz), which is most easily observed in Figure 4b as a small decrease in the imaginary impedance Z' . These changes are similar to those reported previously in studies of antibody–antigen binding²¹ and DNA hybridization at silicon surfaces.⁴¹

To test the reversibility of DNA hybridization and denaturation, the surface was denatured by pumping 8.3

(36) Kelley, S. O.; Barton, J. K. *Science* **1999**, *283*, 375.

(37) Kelley, S. O.; Jackson, N. M.; Hill, M. G.; Barton, J. K. *Angew. Chem., Int. Ed.* **1999**, *38*, 941.

(38) Memming, R.; Schwandt, G. *Surf. Sci.* **1966**, *5*, 97.

(39) Memming, R. *Semiconductor Electrochemistry*; Wiley-VCH: Weinheim, Germany, 2000.

(40) Cole, K. S.; Cole, R. H. *J. Chem. Phys.* **1941**, *9*, 341.

(41) Cai, W.; Peck, J.; van der Weide, D.; Hamers, R. J. *Biosens. Bioelectron.* **2003**, *19*, 1013.

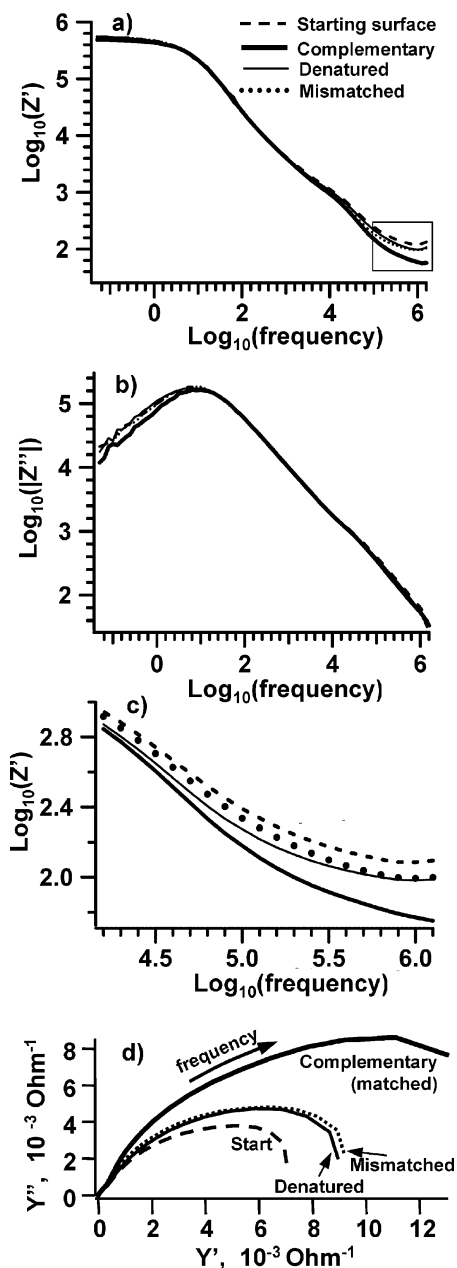


Figure 4. Impedance spectra, measured under open-circuit conditions, of the DNA-modified surfaces at the beginning, after hybridization with a complementary sequence, after being denatured, and after exposure to a mismatched DNA sequence. (a) Real part of the impedance. (b) Imaginary part of the impedance. (c) Magnified view of the real impedance from the region highlighted in panel a. (d) Cole–Cole plot showing real and imaginary parts of the admittance. Points measured at high frequency are farthest to the right, and those measured at lowest frequency occur near the origin.

M urea solution into the cell for 5 min, followed by flushing with HB solution. The impedance moves back toward its original position, although often it does not move back fully to its original value. While the nature of this lack of complete reversibility is yet unclear, experiments probing the effects of urea at intermediate stages of the chemical functionalization process suggest that it arises from urea-induced changes in the molecular layers, rather than any changes in the diamond substrate.

To test the selectivity of DNA hybridization, a solution containing a 5 μM solution of noncomplementary DNA sequence (F2) was then pumped into the cell and incubated for 20 min. The cell was flushed with HB for 10 min, and

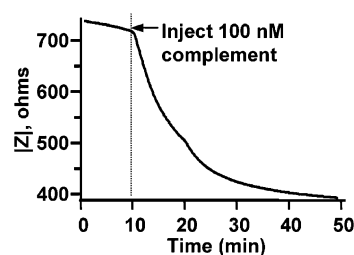


Figure 5. Real-time measurement of the change in total impedance when the DNA-modified surface was exposed to 100 nM complementary DNA.

the impedance spectrum was obtained again. Figure 4 shows that there is very little change in impedance induced by the noncomplementary sequence.

Although not depicted in Figure 4, experiments were conducted in which DNA-modified surfaces were exposed to repeated cycles of exposure to complementary DNA, denatured, and exposed to noncomplementary (mismatched) DNA molecules. These measurements show that exposure to complementary DNA consistently yields a significant decrease in the impedance, while the 4-base mismatched sequence induces no significant change compared with the denatured surface. This trend is observed in all experiments, irrespective of the order in which the measurements are made. The starting surface has the highest impedance (lowest admittance), which increases somewhat with repeated cycles of exposure to the 8.3 M urea used in denaturing. Despite this urea-induced change in the starting impedance, repeated experiments show that exposure to the complementary sequence reduces the total impedance (increases the admittance) by approximately a factor of 1.6–1.8.

Real-Time Measurement of DNA Hybridization.

These data show that at frequencies in the frequency range between ~ 10 kHz and ~ 1 MHz, hybridization induces a significant change in the impedance of the interface. By operating at a fixed frequency of greater than ~ 10 kHz, it is possible to observe the DNA hybridization process on a continuous basis in real time. Figure 5 shows impedance data obtained on a p-type diamond sample that was covalently linked to DNA with sequence S1. The electrical response was measured as a function of time at a frequency of 100 kHz. The standard HB was first flowed through the cell. Starting at $t = 10$ min, a buffer solution with 100 nM complementary DNA, but otherwise identical in composition, was pumped into the system. The total impedance decreased from 710 to 380 Ω over the 50 min duration of the experiment. Fitting the impedance data to a function of the form $Z(t) = Z_0 + \Delta Z[1 - \exp(-t/\tau_{\text{hybrid}})]$ yields a characteristic hybridization time $\tau_{\text{hybrid}} = 8$ min, reaching a final plateau approximately 40 min after injection. At a flow rate of 0.1 mL/min and an internal volume of 4.5 μL , the residence time of solution within the cell is only 0.045 min. Corresponding measurements (not shown) of the fluorescence intensity measured after discrete hybridization times yielded a very similar time dependence. This indicates that the time dependence in Figure 5 is the intrinsic time response of the DNA hybridization process at the surface.

Flat-Band Potential Measurements. To better understand how DNA hybridization influences the electrical properties of the interface, measurements were also performed as a function of the potential of the DNA-modified diamond electrode. Analysis of these data is facilitated by modeling the interface as a simple series resistor R and capacitor C that represent a lumped effective resistance and effective capacitance of the space-

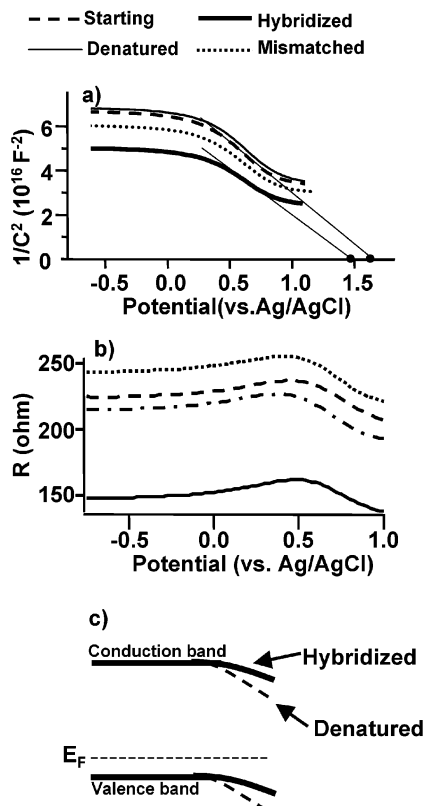


Figure 6. Potential-dependent measurements of the electrical response of DNA-modified diamond surfaces. (a) Mott–Schottky analysis to extract the flat-band potential. (b) Resistance as a function of potential. (c) Schematic illustration showing the change in band-bending induced by DNA hybridization on p-type diamond thin film. The initial surface has the bands bent downward by 1.6 eV. Negatively charged DNA molecules approaching the interface bend the bands upward.

charge region.^{39,42} While in principle the capacitance of the electrical double-layer and the molecular layers also need to be taken into account, detailed analysis (presented below) shows that at the frequency used, the potential-dependent changes in the electrical properties are dominated by the semiconductor space-charge layer. In this case, the data can be analyzed using the Mott–Schottky equation,

$$\frac{1}{C^2} = \frac{2}{\epsilon\epsilon_0 N_d} \left(E - E_{\text{FB}} - \frac{kT}{e} \right)$$

where C is the effective capacitance, ϵ is the dielectric constant of the semiconductor, ϵ_0 is the permittivity of free space, e is the electron charge, N_d is the number density of donors, E is the electrode potential, E_{FB} is the flat-band potential, k is Boltzmann's constant, and T is the temperature.

Figure 6a shows capacitance data (plotted as $1/C^2$ vs potential) as a function of potential for various DNA-modified diamond surfaces, measured at 100 kHz. At all potentials, the capacitance of the hybridized surface is larger than those of the denatured surface and the surface exposed to a mismatched sequence, consistent with our other observations. $1/C^2$ is constant at large negative potentials and linear between ~ 0.2 and 0.7 V and then

reaches a limiting value at higher potentials. The changes in shape as a function of potential are identical to those commonly observed on p-type semiconductors having a low density of surface states.³⁹ The strong potential dependence in Figure 6a indicates that the Fermi level at the surface of the DNA-modified diamond surfaces has a sufficiently low density of surface states that an externally applied potential can easily alter the energy of the valence and conduction bands, producing changes in resistance and capacitance of the diamond space-charge region.

Because the plots in Figure 6a are approximately linear over the potential range from 0.2 to 0.7 V, extrapolating this linear range to $1/C^2 = 0$ and using $kT/e = 26.1$ mV gives the flat-band potential. Our measurements yield a flat-band potential of 1.67 V for the diamond sample modified with sequence S1. This value shifts to 1.47 V after exposure to the complementary sequence, while exposure to the noncomplementary sequence F2 yields a flat-band potential of 1.62 V, close to the original value. Although the extrapolation is subject to significant error, the shift is sufficiently large that we believe it to be well outside the limits of error. The Mott–Schottky analysis indicates that hybridization shifts the flat-band potential in the negative direction.

Figure 6b shows that the effective resistance is nearly constant at negative potentials, shows a small peak at around 0.4 V (vs Ag/AgCl reference electrode), and then decreases as the added potential is reaching the flat-band potential of the diamond. These potential-dependent changes are characteristic of p-type semiconductors³⁹ and are similar to our previous observations on p-type silicon surfaces.²² The pronounced decrease in resistance upon exposure to the complementary DNA sequence is consistent with the results shown in Figure 4, again showing that hybridization decreases the real (resistive) part of the impedance. The small peak near 0.5 V is similar to that observed on other semiconductors and attributed to charging of surface states.^{20,38}

These potential-dependent measurements in Figure 3 and Figure 6 establish a number of important facts. First, the fact that the changes in $1/C^2$ are large and that the shape of the plots of $1/C^2$ and R as a function of potential have the characteristic shape expected for a p-type semiconductor indicates that at the frequencies used the impedance is controlled primarily by the semiconductor space-charge region. Second, they demonstrate that application of an external potential shifts the energies of the conduction and valence bands. This implies that the Fermi level of the diamond is not strongly pinned and that the imposition of an external electric field can change the interfacial impedance significantly. This, in turn, suggests that similar electric fields induced by charged DNA molecules are likely to have significant effects on the electrical properties. Finally, they demonstrate that at the open-circuit potential (typically ca. -0.2 V vs Ag/AgCl), the diamond surface is in depletion. While the complex physical structure of the interface is expected to lead to a complicated electrical behavior, these results indicate that at the high frequencies where the sensitivity to DNA hybridization is observed, the overall impedance is controlled by the diamond space-charge region.

Discussion

Understanding the electrical properties of biologically modified surfaces is important for potential applications such as real-time biological sensing. A number of previous studies have shown that changes in low-frequency conductivity can be used to detect biological binding processes,

(42) Rajeshwar, K. Fundamentals of Semiconductor Electrodes and Photoelectrochemistry. In *Semiconductor Electrodes and Photoelectrochemistry*; Licht, S., Bard, A., Eds.; Wiley-VCH: Weinheim, Germany, 2002; Vol. 6.

especially when facilitated by redox species at or near the interface.^{11,12,43} In those experiments, the signal transduction involves dc conduction through the molecular layers, which can in turn be modified by biological binding at the surface. The addition of redox species at or near the interface is typically used to facilitate the electron transfer.^{11,12,43–47} One potential disadvantage of such methods is that DNA hybrids can be denatured by the relatively large potentials (volts or more) typically applied during the experiments.^{48,49} A number of recent studies from our group⁴¹ and other groups^{18–21} have shown that biological binding at semiconductor surfaces can alter the electrical response through a “field effect”, in which the charge on biological molecules at a surface alters the conductivity in the semiconductor (typically silicon). Because field effects are expected only on semiconducting substrates, such as silicon and diamond, they are not present on substrates such as gold, making the intrinsic electrical response mechanism on semiconductors very different from that of the metallic substrates.

Here, we focus primarily on understanding the electrical properties of DNA-modified diamond using small ac potentials, so that there is no net redox chemistry occurring. We first discuss the electrical properties of diamond surfaces modified with single-stranded DNA in order to understand the principal features that give rise to the overall electrical response. We then address how the electrical properties of DNA-modified diamond are modified by hybridization.

Frequency-Dependent Electrical Response of DNA-Modified Diamond Surfaces. To understand the electrical response and the hybridization-induced changes, the impedance data were analyzed using equivalent circuit models with discrete elements. As depicted in Figure 7a, the interface can be divided into three physical regions: (1) the molecular layer and its associated double-layer, (2) the space-charge layer in the diamond substrate, and (3) the bulk solution. Because the physical boundaries between the layers are not sharp (due, for example, to surface roughness and the finite thickness of the molecular layers), accurate quantitative modeling would require a more complicated, distributed circuit model. The simpler electrical model illustrated in Figure 7a was used because it provides a high-quality fit with only a small number of free parameters and a good connection to the physical interface structure, thereby providing a good qualitative understanding of the electrical properties.

This model consists of a resistance (R_{SOL}) due to uncompensated solution resistance between the reference electrode and the surface, a parallel combination of resistor R_1 and capacitor C_1 , and a parallel combination of resistor R_2 with a constant phase element (CPE2). This model is guided by a physical model, in which R_1 and C_1 reflect the properties of the molecular layers and their associated electrical double-layer (here, interpreted to mean any nonuniform distribution of ions near the interface), and

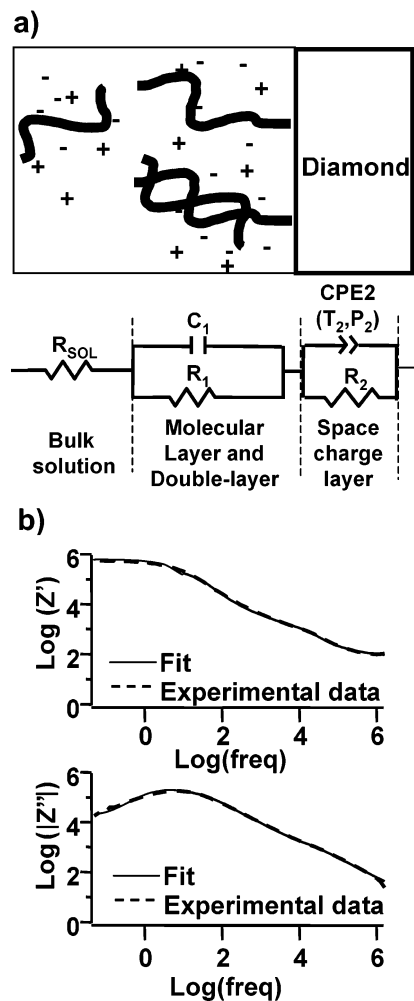


Figure 7. Fitting of impedance data to the electrical circuit model. (a) Simple physical picture of the interface and electrical model used for modeling. (b) Experimental data and resulting fit to the electrical circuit model. Data are shown here for the DNA-modified surface before hybridization. Table 1 gives actual component values for three DNA-modified surfaces.

R_2 and CPE2 reflect the impedance of the diamond space-charge region. The CPE has an impedance defined by

$$Z = \frac{1}{T(i\omega)^P}$$

where T and the exponent P are nonintegral, adjustable parameters.^{50,51} Values of $P < 1$ are often attributed to surface roughness; however, previous studies have found it necessary to include a CPE even on flat single-crystal diamond surfaces and have attributed it to depth-dependent variations in the acceptor concentration arising from hydrogen compensation of subsurface acceptor sites.⁵² We have found it necessary to incorporate a CPE in our model in order to adequately fit our data.

Figure 7b shows one set of experimental data and the resulting fit for a surface modified with single-stranded DNA. In fitting the data, a single set of parameters was used to simultaneously fit the real and imaginary parts of the impedance over the frequency range from 0.1 Hz to 1 MHz. The low χ^2 of 0.004 indicates a very good fit.

(50) Macdonald, J. R.; Kenan, W. R. *Impedance Spectroscopy: Emphasizing Solid Materials and Systems*; J. Wiley: New York, 1987.

(51) Macdonald, J. R. *Solid State Ionics* **1984**, *13*, 147.

(52) Kondo, T.; Honda, K.; Tryk, D. A.; Fujishima, A. *Electrochim. Acta* **2003**, *48*, 2739.

(43) Yu, H.-Z.; Luo, C.-Y.; Sankar, C. G.; Sen, D. *Anal. Chem.* **2003**, *75*, 3902.

(44) Willner, I.; Willner, B. *Trends Biotechnol.* **2001**, *19*, 222.

(45) Patolsky, F.; Weizmann, Y.; Willner, I. *J. Am. Chem. Soc.* **2002**, *124*, 770.

(46) Boon, E. M.; Ceres, D. M.; Drummond, T. G.; Hill, M. G.; Barton, J. K. *Nat. Biotechnol.* **2000**, *18*, 1096.

(47) Bardea, A.; Patolsky, F.; Dagan, A.; Willner, I. *Chem. Commun.* **1999**, 21.

(48) Sosnowski, R. G.; Tu, E.; Butler, W. F.; O'Connell, J. P.; Heller, M. J. *Proc. Natl. Acad. Sci. U.S.A.* **1997**, *94*, 1119.

(49) Heaton, R. J.; Peterson, A. W.; Georgiadis, R. M. *Proc. Natl. Acad. Sci. U.S.A.* **2001**, *98*, 3701.

Table 1. Results of Fitting Experimental Data to the Circuit Model Shown in Figure 7

	R_1 , k Ω	C_1 , nF	R_2 , M Ω	T_2 , 10^{-6}	P_2	R_{SOL} , Ω
denatured	151 \pm 9	75 \pm 5	0.41 \pm 0.01	0.30 \pm 0.02	0.675 \pm 0.005	65 \pm 3
hybridized	95 \pm 9	103 \pm 12	0.40 \pm 0.01	0.18 \pm 0.01	0.724 \pm 0.005	25 \pm 2
mismatch	130 \pm 10	79 \pm 6	0.43 \pm 0.01	0.29 \pm 0.02	0.682 \pm 0.005	49 \pm 3

Similar fitting of the other data sets (not shown) yields similarly good agreement. Table 1 shows the resulting fit parameters for a DNA-modified diamond sample before and after exposure to complementary DNA and for a denatured sample that was then exposed to a mismatched sequence.

Detailed analysis of the circuit modeling results shows that at low frequencies (<10 Hz), the impedance is dominated by R_1 and R_2 , which have similar values. In this range, the small imaginary part of the impedance arises primarily from CPE2. As the frequency increases above 10 Hz, the impedance associated with C_1 , CPE2, and the total impedance all decrease. Between 10 Hz and 1 kHz, the impedances of R_1 , C_1 , and CPE2 are similar, so no single element dominates the total impedance. However, because the exponent P_2 in the CPE element is less than 1, as the frequency is increased the impedance of CPE2 decreases less quickly than that associated with C_1 . Consequently, at higher frequencies the impedance becomes dominated by CPE2; as the frequency approaches 10^4 Hz the total impedance of CPE2 becomes approximately 10 times that of C_1 , and at $f > 10^4$ Hz CPE2 dominates the impedance of the system. As the frequency approaches the highest values used (1.6 MHz), the uncompensated solution resistance R_{SOL} becomes significant.

Thus, we conclude that for frequencies below ~ 10 Hz, Z is dominated by R_1 and R_2 , and the smaller Z' is controlled primarily by CPE2. For frequencies above 10 Hz, the impedance becomes dominated by C_1 and CPE2, and for 10^4 Hz $< f < 10^6$ Hz, CPE2 dominates. Finally, as the frequency approaches 1 MHz, the solution resistance is expected to dominate.

An important comparison can be made between the circuit modeling results of the frequency dependence and the Mott–Schottky analysis of the potential dependence. The potential-dependent impedance spectra (Figure 3) and Mott–Schottky analysis (Figure 6) show that at 10^5 Hz, the system exhibits behavior that is characteristic of a pure p-type semiconductor. Circuit modeling of the impedance spectroscopy data shows that at this same frequency, the impedance is clearly dominated by CPE2. This comparison establishes a strong link between the electrical and physical models of the interface, by showing that CPE2 does indeed arise from the diamond space-charge region. It is also in agreement with previous studies that have shown that at semiconductor–electrolyte interfaces, the capacitance of the double-layer is larger than the capacitance of the semiconductor space-charge layer, so that the impedance is typically dominated by the semiconductor.^{18,42,53}

Hybridization-Induced Impedance Changes. In principle, there are a number of ways in which DNA hybridization can affect the electrical properties of the interface (see, for example, the recent review by Lucarelli et al.⁵⁴). These include increased conductivity of the DNA layers,^{36,37,55} changes in capacitance of the biomolecular layers,^{18,56} blocking of diffusion near the electrode sur-

face,⁵⁷ and modification of the electronic properties of the semiconductor (here, diamond) space-charge layer via the electric field induced by the hybridizing DNA molecules.^{18–20,22}

While previous studies have shown that DNA is more conductive in its double-stranded form (i.e., after hybridization with a complementary sequence) than in its single-stranded form,^{36,37,55} we observe no significant change in Z (the total interfacial resistance) at very low frequencies, and our cyclic voltammetry results also show almost no change. This result is not surprising, because in our experiments the DNA molecules that were tethered to the surface included a repeated sequence of 15 thymine groups that were not involved in hybridization, as depicted in Figure 1b. Thus, even though the hybridizing region may be becoming more conductive,^{36,37,55} the insulating properties of the remainder of the molecule and the molecular scaffolding used to tether the DNA to the surface render the overall assembly so highly insulating that the change in total resistance is not easily detected. Nevertheless, the influence of hybridization on the electrical properties can be identified through frequency-dependent measurements at higher frequencies. For example, studies of antibody–antigen interactions on oxidized silicon surfaces showed sensitivity to binding that was most sensitively detected near 100 kHz;²¹ the hybridization changes were most pronounced in the real part of the impedance and smaller in the imaginary part, in close agreement to our more recent results on silicon surfaces⁴¹ and the results we report here on diamond.

Our impedance spectroscopy measurements show that the most significant hybridization-induced changes in impedance occur at frequencies between approximately 10^4 and 10^6 Hz. This corresponds roughly to the same range of frequencies over which the potential-dependent measurements (Figure 3) show a large dependence on potential. The flat-band potential measurements (Figure 6) made within this range, at 10^5 Hz, show all the pronounced features normally associated with band-bending in a p-type semiconductor. We note in particular that they show that at the open-circuit potential the diamond surface is in depletion, with an downward band-bending of approximately 1.6 V, and that changes in potential are able to alter the valence and conduction band energies (to “bend the bands”). These factors, together with the impedance modeling results, lead us to conclude that the high-frequency sensitivity arises primarily from the field effect, in which hybridization with complementary DNA brings additional negative charges near the surface, bending the bands upward from their original (depleted) position, closer to the flat-band condition. Because the resistance is smaller and capacitance is larger when the bands are flat, the upward shift in the surface bands induced by the DNA hybridization is expected to decrease the impedance of the diamond space-charge region. The influence of DNA approaching the surface is similar to that observed when a positive potential is applied to the bulk (Figure 3b); in both cases the bands are bent upward near the surface, thereby decreasing the impedance.

(53) Singh, P.; Singh, R.; Gate, R.; Rajeshwar, K.; DuBow, J. *J. Appl. Phys.* **1980**, *51*, 6286.

(54) Lucarelli, F.; Marrazza, G.; Turner, A. P. F.; Mascini, M. *Biosens. Bioelectron.* **2004**, *19*, 515.

(55) Schuster, G. B. *Acc. Chem. Res.* **2000**, *33*, 253.

(56) Berggren, C.; Stalhandske, P.; Brundell, J.; Johansson, G. *Electroanalysis* **1999**, *11*, 156.

(57) Hianik, T.; Gajdos, V.; Krivanek, R.; Oretskaya, T.; Meteleev, V.; Volkov, E.; Vadgama, P. *Bioelectrochemistry* **2001**, *53*, 199.

Our conclusion that the sensitivity to DNA hybridization occurs primarily via a field effect is further supported by previous results on n-type ultrananocrystalline diamond⁵⁸ samples (not shown) and by measurements on DNA-modified surfaces of p-type and n-type silicon.^{18,20,21,41} On n-type diamond samples covalently modified with DNA, we observed an increase in impedance upon hybridization; if it is assumed that n-type diamond is also in depletion with an upward band-bending, then one would expect the direction of impedance change to be opposite on p-type and n-type samples, in agreement with our observations. Similarly, we have recently found that when silicon surfaces that were covalently modified with DNA were exposed to complementary DNA, the high-frequency impedance decreased when p-type Si substrates were used and increased when n-type substrates were used.²² Negative shifts in flat-band potential for DNA immobilized onto Si surfaces and concurrent decreases in impedance upon hybridization on p-type silicon have also been reported previously.^{18,20} All these measurements point to a common mechanism in which the negative charge associated with DNA induces a field effect into the underlying semiconductor substrate, with commensurate changes in resistance and capacitance of the space-charge region.

These conclusions can be connected to the circuit modeling presented above. Table 1 shows that hybridization affects the values of all the circuit elements, but an analysis shows that the most significant effect is on CPE2. The prefactor (T_2) is slightly smaller on the hybridized surface, leading to the slight reduction in Z' upon hybridization visible at $f < 10$ Hz in Figure 4b. The more significant effect of hybridization, however, is to decrease the exponent P_2 of CPE2, which makes the impedance of CPE2 decrease more slowly at high frequencies. We also observe an increase in capacitance C_1 and a decrease in resistance R_1 . We associate R_1 and C_1 with the molecular layers; the increase in C_1 and decrease in R_1 suggest that there may be some increased density of ionic charges at the interface after DNA hybridization. Our fitting also shows a small change in the value of R_{SOL} . Based on the bulk conductivity of $3.1 \Omega^{-1} \text{ m}^{-1}$ and the physical dimensions of our electrochemical cell, we anticipate an uncompensated solution resistance of 53Ω . Because the hybridization-induced changes in R_{SOL} are quite small, their value depends on the impedance at the extreme high-frequency limit of the impedance instrumentation; consequently, it is not clear if the differences in R_{SOL} are real or whether they result from limitations of apparatus and the circuit model. The increase in capacitance C_1 and decrease in resistance R_1 suggest that hybridization induces some measurable changes in the electrical properties of the molecular layers. Because R_1 and C_1 are lumped quantities representing the total response of the functionalization layer, the SSMCC linker, and the DNA oligonucleotides, it is difficult to assign these changes to one specific molecular response. However, since DNA hybridization and the associated DNA duplex formation involve substantial changes in molecular structure, changes in resistance and capacitance are not unexpected. Previous impedance spectroscopy studies of DNA hybridization immobilized on conductive surfaces such as conductive polymers have also reported that hybridization decreases the impedance, with a maximum sensitivity reported near 1 kHz.⁵⁹

DNA-Induced Field Effect and Surface Charge Density. Our data show that the hybridization-induced

changes in impedance observed at high frequencies arise primarily from a field effect in which the negative charge of DNA molecules hybridizing with their surface-bound complements induces an upward band-bending in the diamond space-charge region. The size of this field effect (and the resulting change in impedance of the diamond) is controlled by a number of different factors. Previous studies of semiconductor–electrolyte interfaces have shown that the capacitance associated with the ions in solution (the double-layer) is typically much larger than the capacitance associated with the semiconductor space-charge region.^{42,53} Consequently, specific adsorption of ions at the interface leads to significant changes in potential within the semiconductor but only small changes in potential within the electrolyte solution. If it is assumed that the diamond Fermi level is unpinned and the potential drop within the aqueous solution can be ignored, then the flat-band potential can be used to determine the number of effective charges at the surface. Using the depletion approximation, the surface charge density is given by

$$\sigma_{\text{surface}} = \sqrt{\frac{2\kappa\epsilon_0 N_A V}{q}}$$

where σ_{surface} is the number of charges per unit area, N_A is the concentration of acceptors, and V is the change in potential between surface and bulk, also referred to as the “band-bending”. Subtracting the surface charge density before and after hybridization (using $V = 1.67$ and 1.47) leads to the conclusion that the charge density within the semiconductor bulk changes by $\sim 3 \times 10^{11}$ electrons/cm² upon DNA hybridization. We have determined previously²⁴ that the number density of DNA molecules hybridized to the diamond surface is approximately 3×10^{12} molecules/cm², with each DNA molecule carrying multiple negative charges.

The above analysis shows that the total change in charge within the space-charge layer is significantly smaller than the charge associated with the hybridizing DNA molecules. We believe this has three possible origins. First, we note that the negative charge on the DNA backbone is partially compensated by loosely bound cations; however, this is expected to reduce the charge by no more than a factor of 2 from its bare value.⁶⁰ A second contributing factor is that surface states at the semiconductor–electrolyte interface (such as unterminated surface “dangling bonds”) can screen the diamond from the negative charge of the hybridizing DNA molecules, thereby reducing the field effect. In Figure 6b, the small peak in the real part of the impedance is similar to that reported previously on modified silicon surfaces and attributed to charging of surface states.^{20,38} However, our Mott–Schottky plots suggest that the effect of these surface states must be fairly small, since we clearly observe the change from depletion to flat-band and then to slight accumulation as the potential is made more positive. Finally, because the DNA molecules are separated from the diamond surface by a set of molecular linkers consisting of the amine-terminated alkyl chain and the SSMCC linker, it is likely that DNA hybridization induces significant charge redistribution within the double-layer and within the molecular linking layers itself. Changes in the interstitial water and ions within this region could significantly screen the effect of the DNA molecules, thereby reducing the overall magnitude of the field effect.

(58) Gruen, M. D. *Annu. Rev. Mater. Sci.* **1999**, *29*, 211.

(59) Lee, T.-Y.; Shim, Y.-B. *Anal. Chem.* **2001**, *73*, 5629.

(60) Rasmusson, M.; Akerman, B. *Langmuir* **1998**, *14*, 3512.

Conclusions

Our experiments show hybridization of DNA induces a significant field effect in diamond thin films and that these changes can in turn be used as a real-time, label-free, sequence-specific method for detecting DNA molecules in solution. Our previous measurements using fluorescence as a basis for observing DNA hybridization at diamond thin films revealed a very good biological selectivity and excellent chemical stability.^{23,24} The present electrical measurements likewise show that the modified films have a low surface state density that permits the charged biomolecules to induce a significant field effect in the diamond film. While denaturation in urea induces some changes in the electrical properties, these changes likely occur in the molecular layer. Clearly, field-effect electrical measurements may be particularly sensitive to unintended alteration of the charge distribution within the molecular layers, and electrical biosensors using the field effect for signal transduction will require an even greater degree

of control over the interface chemistry in order to achieve their full potential. Yet, the present results demonstrate that diamond surfaces covalently modified with DNA have sufficiently low surface state densities that the field effect can be easily detected using impedance spectroscopy and establish that it is possible to create field-effect biological sensors on diamond thin films.

Acknowledgment. This work was supported in part by the Wisconsin Alumni Research Foundation, National Science Foundation Grants CHE0314618 and BES03-30257, the U.S. Office of Naval Research, and the U.S. Naval Research Laboratory.

Supporting Information Available: Frequency-dependent impedance measurements in the presence and absence of added redox agent. This material is available free of charge via the Internet at <http://pubs.acs.org>.

LA036460Y